Trends in Cardiovascular Medicine xxx (xxxx) xxx

Contents lists available at ScienceDirect

Trends in Cardiovascular Medicine

journal homepage: www.elsevier.com/locate/tcm

Evaluation of aortic stenosis: From Bernoulli and Doppler to Navier-Stokes

Harminder Gill[a,*], Joao Fernandes[a], Omar Chehab[b], Bernard Prendergast[b], Simon Redwood[b], Amedeo Chiribiri[a], David Nordsletten[a,c], Ronak Rajani[a,b], Pablo Lamata[a]

[a] School of Biomedical Engineering and Imaging Sciences, King's College London, London, UK
[b] Cardiology Department, Guy's and St. Thomas's Hospital NHS Foundation Trust, London, UK
[c] Department of Surgery and Biomedical Engineering, University of Michigan, 2800 Plymouth Rd, 48109, Ann Arbor, MI, USA

ARTICLE INFO

Keywords:
Aortic stenosis
Pressure drop
4D flow MRI
Velocity vector ultrasound

ABSTRACT

Uni-dimensional Doppler echocardiography data provide the mainstay of quantative assessment of aortic stenosis, with the transvalvular pressure drop a key indicator of haemodynamic burden. Sophisticated methods of obtaining velocity data, combined with improved computational analysis, are facilitating increasingly robust and reproducible measurement. Imaging modalities which permit acquisition of three-dimensional blood velocity vector fields enable angle-independent valve interrogation and calculation of enhanced measures of the transvalvular pressure drop. This manuscript clarifies the fundamental principles of physics that underpin the evaluation of aortic stenosis and explores modern techniques that may provide more accurate means to grade aortic stenosis and inform appropriate management.

Introduction

Aortic stenosis (AS) is characterised by progressive thickening and calcification of the aortic valve leaflets resulting in restricted leaflet excursion and obstruction of cardiac output [1]. Studies report a high prevalence of AS (3.9% in the 70-79 year old age group) and a rising incidence in aging populations [2,3]. In the setting of impeded blood flow, the ventricle experiences an increased demand to generate pressures capable of propelling blood across the narrowed valve orifice [2]. Consequently, a number of maladaptations at the microscopic level summate to cause left ventricular (LV) remodelling and eventual impairment [4]. Depressed systolic function heralds a late stage of disease, and is associated with poor outcomes [5]. The mainstay of treatment is surgical or transcatheter valve replacement with the severity of AS governing the need and timing of intervention [6,7].

AS manifests as angina, syncope and dyspnoea, with each additional symptom suggestive of increasingly advanced disease [8]. However, reported symptoms are not universally indicative of disease severity and asymptomatic patients may have haemodynamically significant disease [1]. Clinical examination may identify the pathology, but is insufficiently sensitive to grade disease severity [1]. Therefore, quantifiable measures of valve haemodynamics are essential to substantiate decision-making. In many cases grading the severity of AS is complex, and several factors are assessed in combination.

Assessing the severity of AS

Whilst symptomatic status and presence of LV impairment are dichotomised into binary outcomes, AS severity is categorised based on quantifiable metrics. Historically, retrograde LV catheterisation yielding a "peak-to-peak gradient" and orifice area by the Gorlin (or Hakki) method provided such metrics with the associated risks of haemorrhage, stroke, vascular injury, and exposure to ionising radiation [9,10]. As such, catherization is reserved for cases where uncertainty remains after intensive investigation [6,7]. Non-invasive haemodynamic and anatomic biomarkers of AS severity acquired from echocardiography are the current standard practice (Table 1). In earlier guidelines, Doppler Echocardiography (DE)-derived aortic valve area (AVA) $<$1.0cm [2] or body surface area (BSA)-indexed valve area $<0.6 cm^2/m^2$ alone denoted severe AS [11]. One study of 16,156 echocardiograms with AVA $<$ 1.5cm [2] demonstrated an absence of ventricular outflow obstruction in 12.4% subjects, a finding supported by subsequent larger scale studies, indicating the pitfalls of assigning severity using this metric in isolation [12–14]. Contemporary guidelines emphasise combined evaluation using anatomic and haemodynamic measures of disease severity with transaortic velocity (V_{max}) $>$4m/s or a mean

* Corresponding author at: Department of Biomedical Engineering and Imaging Sciences, King's College London, 5th Floor Becket House, 1 Lambeth Palace Road, London SE1 7EU UK.
E-mail address: harminder.gill@kcl.ac.uk (H. Gill).

https://doi.org/10.1016/j.tcm.2021.12.003
1050-1738/

Table 1
Doppler echocardiographic markers of disease severity.

Parameter	Advantages	Disadvantages
Peak aortic velocity	- direct measurement - evidence base	- potential inaccuracy due to probe alignment
Peak pressure drop	- easy to calculate	- potential inaccuracy due to probe alignment, with potential for amplification of inaccuracy due to squared velocity term. - potential for miscalculation if elevated LVOT velocities are encountered - negates pressure recovery
Mean pressure drop	- evidence base - correlation with invasive peak-to-peak pressure drops	- potential inaccuracy due to probe alignment - negates pressure recovery
Effective orifice area	- less flow-dependent measure of obstruction - evidence base	- potential inaccuracy due to probe alignment - potential inaccuracy due to LVOT diameter measurement - calculated value
Dimensionless Index	- overcomes difficulty of LVOT measurement	- limited evidence base
Energy Loss Index	- accounts for pressure recovery	- potential inaccuracy due to probe alignment - calculated value - additional complexity

Abbreviations: LVOT – left ventricular outflow tract

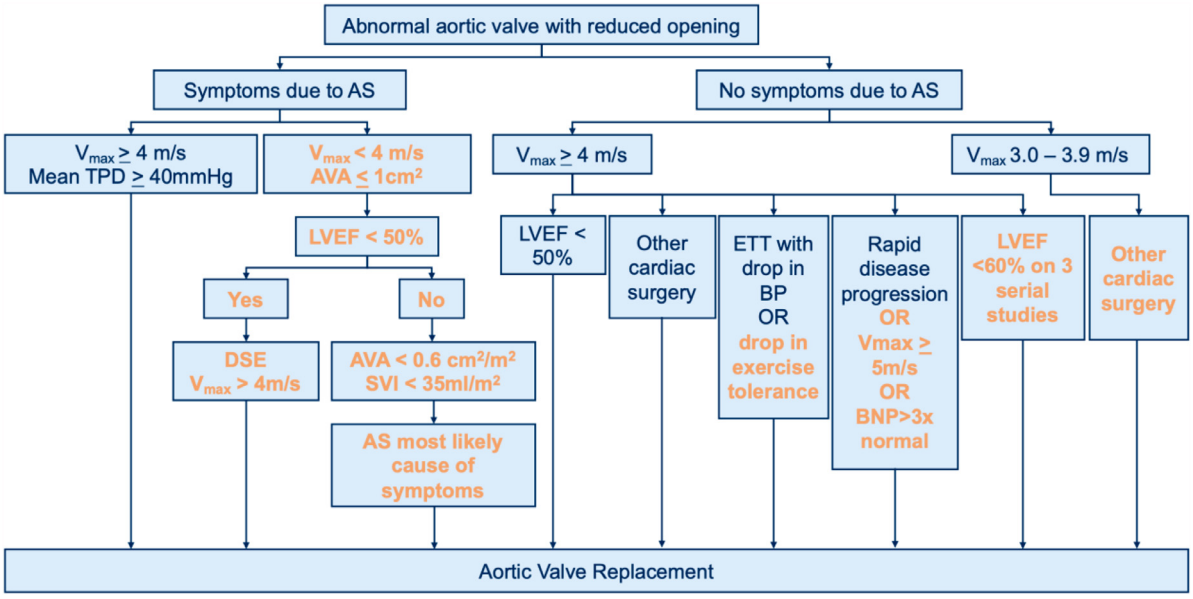

Fig. 1. Changes in the assessment of aortic stenosis. Adapted and simplified 2020 ACC/AHA Aortic Valve Management Algorithm. Additional management steps, when compared with the 2006 guidelines are highlighted in orange.(7,17) Abbreviations: AS – aortic stenosis, AVA – aortic valve area, BNP – brain natriuretic peptide, BP – blood pressure, DSE – dobutamine stress echocardiogram, ETT – exercise tolerance test, LVEF – left ventricular ejection fraction, SVI – stroke volume index, TPD – transvalvular pressure drop, V_{max} – peak jet velocity

transvalvular gradient of >40mmHg denoting severe AS (Figure 1) [6,7].

Retrospective registry data have demonstrated that nearly 60% of patients are asymptomatic despite having severe AS diagnosed by conventional methods [15], a finding that justifies judicious use of exercise stress testing to unmask symptoms where activity levels are subconsciously or deliberately reduced [16,17]. Discordance between Doppler-derived metrics exists in up to 30% of patients [18,19]. Invasive measurements are similarly prone to inconsistent grading with 25% exhibiting disagreement between catheter-derived pressure drops and valve areas, a finding more common in individuals with reduced stroke volume [20]. Guidelines now place greater emphasis on thorough assessment of LV function. Dobutamine-stress echocardiography (DSE) facilitates assessment of the Transvalvular Pressure Drop (TPD) at baseline and under inotrope-stimulation whilst also yielding measures of contractile (or "flow") reserve allowing further differentiation of severe AS in the context of myocardial function [21]. Sub-categories include true severe, low-flow low-gradient severe and pseudo-low flow low-gradient AS [22] (see table 2). Expansion of this classification highlights the heterogeneity of the underlying pathology and the need for increasingly sophisticated assessment.

In some cases, surrogate biomarkers of severity are assessed where categorisation proves challenging based on conventional metrics. For example, valve calcification on cardiac CT (quantified by an Agatston score >1274 units for women and >2065 units for men) is a useful discriminator for identifying severe AS and provides valuable prognostic data [19]. Serum biomarkers, for instance brain natruiuretic peptide (BNP) indicative of myocardial stretch, stratify symptom-free survival and outcomes, and are included in guidelines [6,7].

Ultimately, more accurate and reproducible measures for assigning severity of AS are needed. Indeed, alternative methods for grading the severity of AS have garnered interest but are yet to demonstrate utility beyond conventional techniques [23].

Fundamental physical principles

Despite discordant echocardiographic markers of AS severity and different haemodynamic states associated with AS, clear cut-

Table 2
Biomarkers used for classification of discordant AS.

Parameter	True Severe	Low flow, low gradient	Pseudo- low flow, low gradient
Aortic Valve Area/cm^2 /Indexed cm^2/m^2	≤1.0/≤0.6	≤1.0/≤0.6	≤1.0/≤0.6
Peak aortic velocity/m/s	>4	<4	<4
Mean Pressure Drop/mmHg	>40	<40	<40
Stroke Volume Index/ ml/m^2	>35	<35	<35
Augmentation of flow parameters under inotropic stimulation	NA	Yes	No

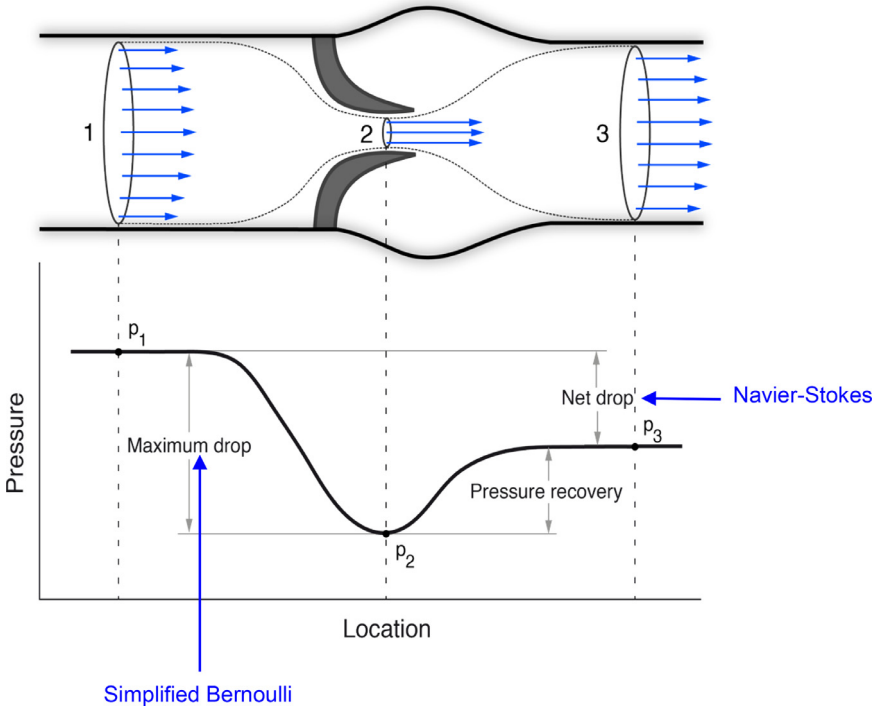

Fig. 2. The physics of the transvalvular pressure drop. Schematic diagram of cross-sectional flow past a stenosis demonstrating the concepts of the maximum drop (measured by the Bernoulli equation) and net drop (measured by the Navier-Stokes equation). The peak velocity measurement made at the vena contracta (P2) yields the peak pressure drop, whereas further downstream the fully recovered pressure, inclusive of the irreversible losses is described by the net pressure drop (P3).* *Adapted from Donati F Thesis: Non-Invasive Relative Pressure Estimation using 4D Flow MRI 2016.

off points are indicated in international guidelines to guide decision making for AVR. This leads one to consider how these physics based parameters are derived and whether in the contemporary era they can be improved upon to enable better risk stratification.

When a body of fluid flows past a constriction, momentum is conserved: spatial acceleration causes energy transfer from potential into kinetic energy, resulting in a pressure drop (Figure 2). Beyond the narrowing (where vessel cross sectional area increases), the fluid decelerates and kinetic energy is partially returned into pressure energy density – a phenomenon known as pressure recovery (position 3 on Figure 2) [24]. Blood velocity can be measured at the vena contracta (point of maximum convergence - position 2 on Figure 2) and application of either the Bernoulli or Navier-Stokes equations allows calculation of the pressure drop [25].

Net versus peak pressure drop

Application of the Bernoulli formula to the peak velocity recorded at the vena contracta yields the *peak TPD*, which accounts for the gain in kinetic energy but not the irreversible energy loss which occurs distal to the vena contracta. The *net TPD* refers to the pressure drop after complete pressure recovery, i.e. after irreversible losses have occurred. Instantaneous differences of pressure transduction obtained by cardiac catheterisation yields a direct measure of the net TPD and is clinically robust despite challenges associated with transducer positioning for complete pressure recovery, oscillation in pressure measurement, and patient volume status [26,27].

The peak TPD is thus a surrogate of the true burden that has demonstrated to be practical and useful, with excellent levels of correlation with peak-to-peak TPDs [28] and successful AS severity grading in clinical guidelines [29] . However, experimental evidence has suggested that the irreversible energy loss (i.e secondary to friction) represented by the net TPD best assesses the additional haemodynamic burden of stenosis [30]. Therefore, correction of routinely acquired metrics to incorporate pressure recovery have been proposed. One such example is the energy loss index (ELI) [31] which demonstrated additional prognosticating power in prospective evaluation of 1873 asymptomatic AS patients from the **S**imvastatin and **E**zetimibe in **A**ortic **S**tenosis (SEAS) [32]. Of note, the ELI was a predictor of combined aortic valve events (aortic valve replacement, hospitalization for heart failure resulting from AS progression, and cardiovascular death) independent of peak aortic velocity or mean aortic gradient [32].

The Bernoulli equation

The Bernoulli equation is used to compute the peak pressure difference from velocity data. It is a simplification of the Navier-

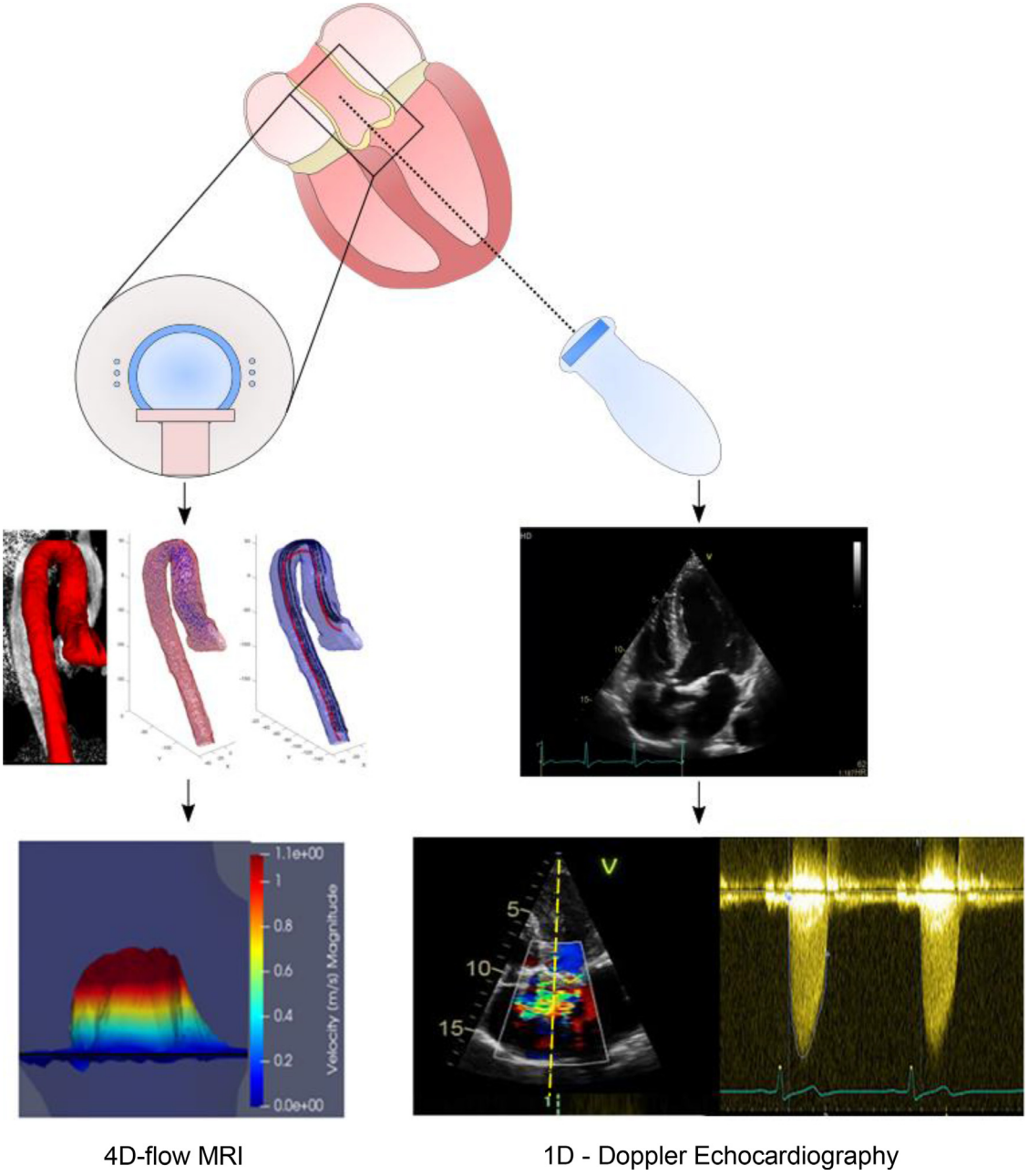

Fig. 3. Velocity data for transvalvular pressure drop calculation. Schematic diagram demonstrating the different approaches to velocity data acquisition. In the case of the conventional Doppler Echocardiography this involves 2D-image acquisition, followed by uni-dimensional velocity acquisition using continuous wave Doppler (right). This is compared with 4D-Flow MRI, where initial gated-acquisition is followed by processing which yields aortic segmentation with a centreline. From this individual velocity vectors across the region of interest can be visualised, giving a 3D representation of blood flow (left). Naturally more data can be input to calculate TPD using 4D-flow MRI and thus estimations should demonstrate improved accuracy. Moreover, being an angle-independent technique it is less prone to interobserver variability as observed with transthoracic echocardiography. Abbreviations: 2D – two dimensional, 3D – three dimensional, 4D-flow MRI – four dimensional flow magnetic resonance imaging, TPD – transvalvular pressure drop

Stokes equation by considering a single, unidimensional streamline of flow [33], and formulates the pressure drop ΔP between points 1 and 2 of a streamline S as (equation 1):

$$\Delta P = p_2 - p_1 = \frac{\rho}{2}\left(V_2^2 - V_1^2\right) + \int_1^2 \frac{dv}{dt} ds + R(\mathrm{v}) \qquad (1)$$

The pressure drop is determined by the addition of 3 components: the spatial (i.e. convective) acceleration resulting from the product of mass density and the velocity change $[\frac{\rho}{2}(V_2^2 - V_1^2)]$, the temporal (i.e. unsteady or kinetic) acceleration $[\int_1^2 \frac{dv}{dt} ds]$ and the viscous losses $[R(\mathrm{v})]$. Viscous energy losses account for the dissipation resulting from friction, either laminar or turbulent. Laminar losses result from the friction between parallel planes of fluid, whereas turbulent losses occur where laminar flow breaks down into vortices, helices and eddy type currents.

Evidence has demonstrated that in AS convective acceleration is responsible for the largest component of the TPD [34]. Therefore, the equation was modified into a format omitting the terms for temporal acceleration $[\int_1^2 \frac{dv}{dt} ds]$ and the viscous component $[R(\mathrm{v})]$,

as:

$$|\Delta P = p_2 - p_1 = \frac{\rho}{2}\left(V_2^2 - V_1^2\right) \quad (2)$$

The modified Bernoulli (equation 2) is used when LVOT blood velocity is >1 m/s – conditions seldom encountered within a healthy ventricle, but which may be present under pathological obstruction to outflow (as in hypertrophic cardiomyopathy) [35]. In most situations, the equation can be further simplified by omission of the LVOT velocity term [V_1^2] leading to the Simplified Bernoulli (SB) equation [35]:

$$\Delta p = \frac{\rho}{2} v^2 \quad (3)$$

The mean pressure drop is also derived from DE using the SB equation and reflects the difference between LV and aortic pressure throughout systole (see equation 4), where [V_p] is the peak systolic velocity and [V_m] the mean systolic velocity [36]:

$$\Delta P_m = 8V_m^2\left[\frac{V_p}{V_p + V_m}\right] \quad (4)$$

Simplified Bernoulli in clinical practice

In clinical practice, measuring the relative shift in frequency of reflected ultrasound waves permits calculation of velocity using the Doppler effect, facilitating computation of the instantaneous peak TPD and mean TPD via the SB equation [35]. Peak velocity is an independent predictor of outcome and strongly associated with mortality [37]. The mean TPD has significant diagnostic importance, correlating well with catheter-derived TPDs and adverse clinical outcome [38,39].

The assumptions intrinsic for the application of SB pressure drops are not unreasonable. The temporal acceleration component in Eq.1 is omitted, negating the pulsatile nature of physiological blood flow and assuming steady flow [40,41] but this is inconsequential as the temporal acceleration is null at the time of maximum constriction (instantaneous peak drop), and positive acceleration is compensated by the negative acceleration when computing the average drop [42]. Moreover, higher peak aortic jet velocities observed in AS yield a pressure drop which is determined by the convective rather than temporal acceleration [40]. Notably, a highly-controlled phantom circuit has been used to demonstrate stronger correlations with SB-derived peak pressure drops compared with catheter against a ground truth computational fluid dynamics (CFD) solution, demonstrating improved correlation using SB calculations [33]. The ease at which DE and SB can be used to yield TPD drops, whilst standing on a firm evidence base, justifies the continued use of the technique for first-line evaluation of AS.

Nevertheless, over-simplification of the physics and methodological limitations of acquiring velocity data both contribute to the limitations of SB. SB assumes an ideal system where energetic losses are ignored, whereas turbulent dissipation, frequently encountered distal to stenotic and bicuspid valves, has independent stratification value [43]. Thus, the energy losses that are true cause of the additional haemodynamic burden are overlooked [32,44,45].

The tendency of SB to yield overestimated peak TPDs when compared with invasive measurements is widely recognised. The difference can be explained by the requisite assumption that the entire velocity field (i.e. all the velocity vectors across the valve cross section) have a magnitude equal to the peak velocity, whereas in reality, the velocity field is heterogenous [41]. Moreover, the velocity-based technique yields an instantaneous TPD and the catheter measures the pressure drop at two distinct time points (peak to peak).

Technical aspects impact the quality of DE velocity acquisition. Peak velocity measurement requires alignment of incident continuous wave (CW) Doppler beam to interrogate a single streamline of maximal identified flow [41]. Incorrect alignment may result in substantial underestimation of velocity and it is possible for the maximum velocity to be missed altogether. In the clinical setting, up to 15^0 of angulation between the incident beam and maximal jet is permissible, resulting in a 5% underestimation of the true value [35]. Sampling the streamline from CW Doppler yields the uni-dimensional peak jet velocity, disregarding the three-dimensional (3D) blood flow across the valve [46]. Moreover, eccentric jets observed across severely calcified or bicuspid valves may prove challenging to characterise on 2D echocardiography elevating the risk of discordant measurements and incorrect estimation of TPD [47,48]. Difficulties in obtaining diagnostic sonographic windows is a further challenge, especially in elderly cohorts where AS is most prevalent [49].

Strategies to maximise accuracy of the measurement include repeated samples in multiple sonographic windows (the apical window with supplementary suprasternal and right parasternal views) to ensure a true measure of maximal jet velocity [48]. Current guidelines also advise additional data acquisitions over several heartbeats to allow for beat-to-beat variation, particularly in the setting of arrhythmia. Furthermore, use of dedicated, non-imaging Doppler probes is recommended to ensure that maximal aortic velocity measurements are obtained [48]. Concurrent mitral regurgitation can introduce unwanted interference with this measurement resulting in incorrect grading, and careful evaluation is required to avoid this.

Building on Bernoulli: the Navier-Stokes equation

The physics of blood flow in the large arteries and aortic stenosis is ruled by the incompressible Navier-Stokes equation, which in essence is the 3D extension of Bernoulli's equation (equation 5) [25]:

$$\rho\left[\frac{\delta V}{\delta t} + (\mathrm{V}.\nabla)V\right] = -\nabla P + \rho g + \mu\nabla^2 V \quad (5)$$

Components are analogous to the full Bernoulli equation, with terms for temporal acceleration ($\frac{\delta V}{\delta t}$), convective acceleration ($(\mathrm{V}.\nabla)V$), body forces (ρg) and viscous energy losses ($\mu\nabla^2 V$). With application to AS, body forces consist of changes in gravitation and buoyancy (which are equal and can therefore be omitted) [50]. Convective acceleration is an expression of energy expended to accelerate blood across the stenosed valve which can be reduced to the SB equation used in Doppler-derived peak TPD [33].

The Navier-Stokes equation requires 3D velocity vectors in the entire domain, rather than focusing on a single velocity component of a single streamline in SB. By relying on fewer assumptions, and by accounting for pressure recovery and irreversible pressure loss, more accurate estimation of TPD (and cardiac afterload) is possible (Table 3).

Acquisition of dense velocity fields

Magnetic resonance imaging

Contemporary velocity acquisition is achieved using conventional phase-contrast MRI (PC MRI) and more sophisticated techniques (4D-flow MRI) [51,52].

Flow velocity is proportional to the MR phase signal observed across a gradient magnetic field – the core principle underpinning PC MRI. Commonly used unidirectional 2D PC-MRI is based on the application of two interleaved acquisition sequences which differ only by the amplitude of a "phase-encoding" bipolar gradient perpendicular to the imaging plane, and that allows determination of

Table 3
Key differences between the simplified Bernoulli and Navier-Stokes equations

	Simplified Bernoulli	Navier-Stokes
Flow	Steady	Non-steady (i.e. pulsatile)
Fluid	Inviscid	Viscous
Velocity Data	1D	2D, 3D
Data Acquisition	Doppler Echocardiography, 2D PC-MRI	4D-Flow MRI, velocity vector ultrasound
Pressure Recovery	Neglected	Included
Pressure Drop Estimation	Peak	Net

Abbreviations: 1D- uni-dimensional, 3D – three-dimensional, 2D PC-MRI – 2D phase contrast magnetic resonance imaging, 4D-Flow MRI – four dimensional flow magnetic resonance imaging

the difference (or phase shift) in MR signal between the images. The upper velocity limit that can be recorded (termed velocity encoding, VENC) is pre-defined prior to scanning and relates to the amplitude of the phase-encoding gradient. Subsequent data acquisition yields velocity as a function of the phase shift and VENC. Insufficient VENC may result in aliasing although methods which "unwrap" the data to facilitate analysis exist [53].

Assessment of valve disease demands precise velocity measurement, requiring sampling within the region of interest (ROI) to identify the peak velocity and a VENC threshold exceeding the intended acquisition. Measurements with unidirectional 2D PC-MRI can be affected if the acquisition plane is not orthogonal to the direction of peak flow, similar to the challenges faced with DE. Studies comparing velocities derived from 2D PC-MRI and DE have demonstrated strong correlation ($r=0.95$, $p<0.001$), with values under-estimated using 2D PC-MRI (-11.2% ±10.2, $p<0.001$), probably as a consequence of limitations in slice positioning (a requirement that can be corrected by direct visualisation in echocardiography, but not necessarily within an MRI study) [54]. Moreover, MRI velocity acquisition is limited to one slice, whereas Doppler techniques can sample along the entire line of insonation. Anatomical measures, such as geometric orifice area ascertained using planimetry, effective orifice area using the continuity equation, or accurate LVOT cross sectional area from MRI have been reported with similar results to TTE [55].

Contemporary CMR techniques confer the ability to acquire 3D, cine phase-contrast imaging with three-directional velocity-encoding, a technique commonly termed 4D-flow MRI. The accuracy of data acquired using 4D flow MRI has been validated against gold standard techniques such as invasive catheter measurements in a porcine model [56].

There are substantial advantages to 4D flow MRI-derived velocities. By encoding for velocity in all three directions, slice alignment becomes irrelevant, ensuring maximal velocity is acquired. High intraclass correlation coefficients for peak aortic velocities have been observed for both intraobserver ($r=0.92$, $p<0.0001$) and interobserver ($r=0.88$, $p<0.02$) variability [57]. In one study evaluating peak velocity in patients with AS and healthy volunteers using DE, PC-MRI and 4D-flow MRI, 2D PC-MRI underestimated peak aortic velocity when compared with DE whilst 4D-Flow MRI yielded higher velocities than the other two methods (mean difference from TTE: +16.6 ± 10.5%, $p<0.001$) and significantly improved concordance with mean pressure drop and effective orifice area [54]. Rose et al described a method for obtaining velocity maximal intensity plots in paediatric patients with either bicuspid or unicuspid valves which yielded similar velocities to DE (MIP 4D-Flow MRI 2.056 ± 0.83 vs. DE 2.036 + 0.95 m/s, difference=1.1%, $P<0.2485$), and also confirmed that velocities were underestimated using 2D-PC MRI [58]. In a small cohort ($n=10$) of severe AS patients undergoing TAVI, DE significantly overestimated peak pressure drops (61 ± 32 mmHg, $p<0.0002$) when compared with 4D-flow MRI (54 ± 26 mmHG, $p=0.67$), with ground-truth TPD measured invasively (50 ± 34 mmHg) [59]. This particular case may demonstrate the tendency of SB to overestimate the pressure drop, especially where greater velocities are encountered. In summary, DE may correctly identify peak velocity where insonation is correctly aligned with a coaxial jet, whereas MRI may yield higher values in more technically challenging cases where flow displacement is substantial, or beam-alignment is unsatisfactory.

Computed tomography

Velocity data from CT datasets have been reported with high levels of correlation with 4D-flow MRI [60]. The velocity was computed from retrospective analysis of endocardial deformation and subsequent application of CFD calculation. Despite the capability of higher spatial and temporal resolution, substantial processing power and computation time are requisite for the technique. Clinical applicability of such techniques remains to be seen.

Ultrasound

CW and pulsed wave (PW) Doppler echocardiography are widely used to estimate blood flow velocity in clinical practice. Technological advances now permit acquisition of 2D- and 3D-velocity data using ultrasound (termed "velocity vector ultrasound") [61], though remain limited to carotid vascular or transesophageal echocardiographic (TEE) imaging due to depth penetration and image quality. Some, however, have potential transthoracic application. The techniques use ultra-high frame (UHF) rate echocardiography (>1000 frames per second [fps]) compares to the conventional rate of 50 fps) [62] to obtain these data and are already installed in some clinical systems (e.g. blood speckle imaging (BSI), (GE Vingmed, Horten, Norway) [62]. This technique exploits technology similar to speckle tracking used for the calculation of myocardial strain, wherein a small group of pixels (or "kernels") are identified and tracked. Speckle patterns in BSI are acquired from the blood flow signal rather than the myocardium, and resulting data analysed using a best-match algorithm, with results that correlate well with phase contrast MRI [63,64]. It should be noted that BSI technology yields a 2D representation of velocity vectors that overlay the underlying ultrasound magnitude image. A further contrast-enhanced echocardiographic technique uses speckle decorrelation analysis to yield out-of-plane velocity data from cross sectional imaging, and has been shown to be effective in measuring velocities up to 1m/s in the rabbit aorta that correlate closely with ultrasound imaging velocimetry and invasive catheter measurement [65]. Olesen et al reported successful 2D velocity vector imaging of a healthy aortic valve, but the low resolution images were limited by signal-noise ratio [66]. Aliasing may prove problematic at higher velocities and feasibility of capturing the higher velocities in AS is undergoing evaluation. Further limitations include inadequate tissue penetration and image quality at UHF rate with current transducer technology and substantial processing times for some techniques.

Derivation of pressure drop using 3D velocity vectors

Methods to non-invasively capture the TPD have been described using both computational analysis of acquired velocity data, and other CFD techniques that simulate velocity, as summarised in Table 4. [88,89]

Various components of the full Navier-Stokes equation have been used as surrogate measures of the net TPD from 3D velocity vectors. Accounting for only the spatial acceleration to estimate the peak TPD is the most common choice. The most basic technique involves application of SB to the peak velocity data, thus emulating DE and inheriting the assumptions and limitations of SB formulation, but with 4D flow MRI providing an ability to capture the peak velocity with more certainty [59]. An improved version is to estimate the actual spatial (i.e. convective) acceleration at the point of maximum constriction: by accounting for the velocity profile in the cross section of the lumen at vena contract level, it is possible to correct for a variable overestimation of SB [41], a technique known as the Simplified Advective Work-Energy Relative pressure (SAW).

More intensive approaches focus on quantifying flow inefficiencies. Viscous energy losses due to friction between laminar planes result in dissipation of kinetic energy, and this has been successfully measured non-invasively using PC-MRI [67]. Barker et al described application of a reformulated Navier-Stokes equation to yield viscous dissipation at the individual voxel within a defined ROI facilitating the calculation of net viscous energy loss over time, which demonstrated good correlation with conventional TPD assessment in a small group of patients combined AS and aortic dilatation [67].

Where the pressure drop is large, the greatest share of irreversible energy loss is due to turbulent flow, characterised by irregular fluctuations and mixing, in contrast to the regular and smooth layers of laminar flow. Turbulent flow that serves as a further obstruction to flow itself is frequently present distal to a stenosis and has been demonstrated both experimentally and the human aorta [68,69]. Measurements of turbulent kinetic energy using 4D-flow MRI have been described [70]. Additionally, turbulence intensity using 4D-flow MRI correlates well with assessment using laser particle velocimetry [71,72].

Direct estimation of the net TPD using 4D-Flow MRI requires specialised MRI sequences to acquire all the components of the turbulent dissipation [43,73]. Working with a fixed stenosis phantom, it has been demonstrated using the energy balance equation that turbulent kinetic energy-based estimates of irreversible pressure loss correlate well with computational ground-truth solutions, with substantial improvements over the SB and incremental improvement over the Extended Bernoulli [74]. In the same study, at clinically-practical spatial resolutions, the signal-to-noise ratio did not have a significant impact on the measured pressure drop, although the data were acquired in steady flow conditions. Other groups have compared turbulent kinetic energy measurements in AS patients against the mean TPD, demonstrating no correlation amongst AS patients suggesting this measure captures data distinct from conventional methods [43].

We have described assessment of net TPD using the Work-Energy Relative Pressure (WERP)[75]. This formulation was applied to synthesised aortic coarctation and healthy aorta data demonstrating good correlation with computed ground truth pressures [75]. The Simplified Advective Work [SAW] applies an abbreviated form of the WERP equations to an outlet plane (3D) velocity profile at the level of the vena contracta and delivers improved precision and accuracy [41]. Mathematical development of virtual fields has shown to further improve robustness and accuracy in the estimates in the virtual WERP (vWERP) with further improvement incorporating turbulent energy dissipation (vWERP-t) [76].

Discussion

Categorising the severity of aortic stenosis requires integration of data describing both the degree of valvular obstruction and the response of the ventricle with attention to systemic loading conditions. The current clinical standard of echocardiography represents an accessible, cost effective and pragmatic technique. It is, however, subject to some limitations that clinicians should be aware of. Cardiac magnetic resonance imaging with 4D flow overcomes some of these limitations but is restricted by a lack of large scale validation studies, cost and widespread availability. It remains yet to be established whether it may be useful as an adjunct to echocardiography and if so for what patient populations.

Justification for improved measures of valvular severity is evidenced clinically with both discordance and poor symptomatic correlation, which are a result of methodological and intrinsic limitations of the DE velocity acquisition and the SB equation respectively. Invasive haemodynamic quantification has been long-regarded as the gold-standard for stratification of AS, being a "direct measurement" and accounting for pressure recovery and thus the real burden on the ventricle [77]. Despite early studies indicating a strong correlation between DE-derived instantaneous peak and catheter-derived peak-peak TPDs [78], contemporary reports suggest a more substantial discrepancy exists [79]. Interestingly, the correlation between instantaneous peak and peak-to-peak TPDs was weaker amongst AS patients compared with hypertrophic cardiomyopathy patients (r^2 = 0.69 vs 0.98) demonstrating the difficulty of estimating the net TPD from a peak measurement in AS [80]. Non-invasive measures of the net TPD, without the associated risks of catheterisation, represent an ideal which can now be achieved [76].

Various formulations stemming from the Navier-Stokes equations aim to quantify the net TPD. Laminar viscous losses are a surrogate of the net TPD, but comprise only a minute proportion of overall dissipation and is severely underestimated and dependent on spatial resolution [73]. Pressure mapping undertaken from 4D-flow MRI data has been successfully piloted in patients with bicuspid AV yielding additional haemodynamic quantification above and beyond conventional techniques [81]. Viscous losses due to turbulent effects are the largest component for large net TPDs, and by integrating the turbulent component into the estimation the net TPD can be measured non-invasively from 4D-flow MRI data with excellent accuracy [76].

These increasingly comprehensive computational techniques are envisaged to play a role in the future assessment of AS (figure 4). Whilst DE rightfully remains the primary screening and assessment tool in AS, 4D-flow MRI may complement the assessment of borderline cases and assist clinical decision-making. Particular clinical scenarios where more accurate and detailed information may be helpful include: (A) asymptomatic severe AS where overestimated Doppler gradients may explain the lack of symptoms, (B) non-severe AS with discordant measurements (including bicuspid aortic valves), (C) significant AS in the setting of aortic dilation, a group where the TPD may be underestimated [43], and (D) distinction between low-flow, low gradient AS and pseudo-severe AS as an alternative to stress echocardiography.

Groups have demonstrated feasibility and validated the use of 4D flow MRI in patients with severe AS [59]. 4D-flow MRI–derived SB pressure drops and effective orifice area displayed a superior association to 6-minute walk test and LV mass regression when compared to echocardiography alone [59]. The 3D velocity data from MRI overcome DE limitations by being angle-independent, with potential for increased precision and reproducibility. Coupled with gold-standard myocardial function assessment, accurate aortic anatomy and geometry, a more complete picture of the global afterload and ventricular response is possible. Direct visualisation

Table 4
Non-invasive pressure drop/surrogates from 4D-flow MRI

Author and year	Study Subject	Comparator	Measure of AS severity	Findings/Comments
Dyverfelt et al, 2013[72]	AS n=14, controls n=4	Irreversible pressure loss from energy loss index (ELI). Multiple modalities used.	TKE	TKE strongly correlated with ELI. $R^2 = 0.91$ $P<0.001$. Study demonstrates the relationship between a surrogate of the net TPD and a clinically-validated measure.
Barker et al, 2014[67]	AS n = 14, controls = 12	Max and Net TPD	Viscous Energy losses	Significant correlation between SB ($r2 = 0.86$, $p<0.001$) and ELI ($r2 = 0.91$, $p<0.001$). Interobserver variability mean limit of agreement was 6%.
Casas et al, 2016[88]	CFD-simulated MRI data from a stenotic flow phantom, varying stenosis	Max TPD from SB	Net TPD from EB, Pressure Poisson equation TKE/viscous dissipation	Strong linear correlation between net TPD and SB and EB derived pressure drop. Very strong linear correlation between viscous and turbulent energy loss and net TPD.
Binter et al, 2017[43]	AS n = 55 (severe 27, mild/moderate 24), controls = 10	Doppler Echocardiography – mean pressure gradient, Energy Loss Index	TKE	No significant or only weak correlation between MPG and TKE. Negative correlation with ELI
Ha et al, 2017[74]	Phantom with compliant tubing, fixed valve orifice, steady flow	Computational fluid dynamics ground truth, Extended Bernoulli (EB)	Turbulent Energy Dissipation	Turbulent energy dissipation was better correlated with ground truth CFD solution ($R^2 = 0.999$), improving on that achieved by EB ($R^2 = 0.990$) and SB ($R^2 = 0.991$).
Haralddson et al 2017[89]	rPhantom with rigid pipe, fixed cosine-shaped stenosis	Computational fluid dynamics solution	Reynold Stress Tensor	Identification of Reynolds stress tensor and use of Poisson Pressure Equation (PPE) for pressure loss solution
Donati et al, 2017[41]	Bicuspid aortic valve n = 32	SB and NS from 4D-flow MRI velocities	Simplified Advective Work (SAW)	SAW improves precision and accuracy over SB in the estimation of peak TPD requiring minimal extra time or computation
Marlevi et al, 2020[76]	Stenotic Phantom/in silico	Catheter sensors	Virtual work-energy relative pressure accounting for turbulence (vWERP-t)	vWERP-t showed nearly perfect correlation with ground truth measurements of the net pressure drop .

Abbreviations: AS – aortic stenosis, EB – Extended Bernoulli NS – Navier-Stokes, SB – Simplified Bernoulli, TKE - turbulent kinetic energy, TPD – transvalvular pressure drop,

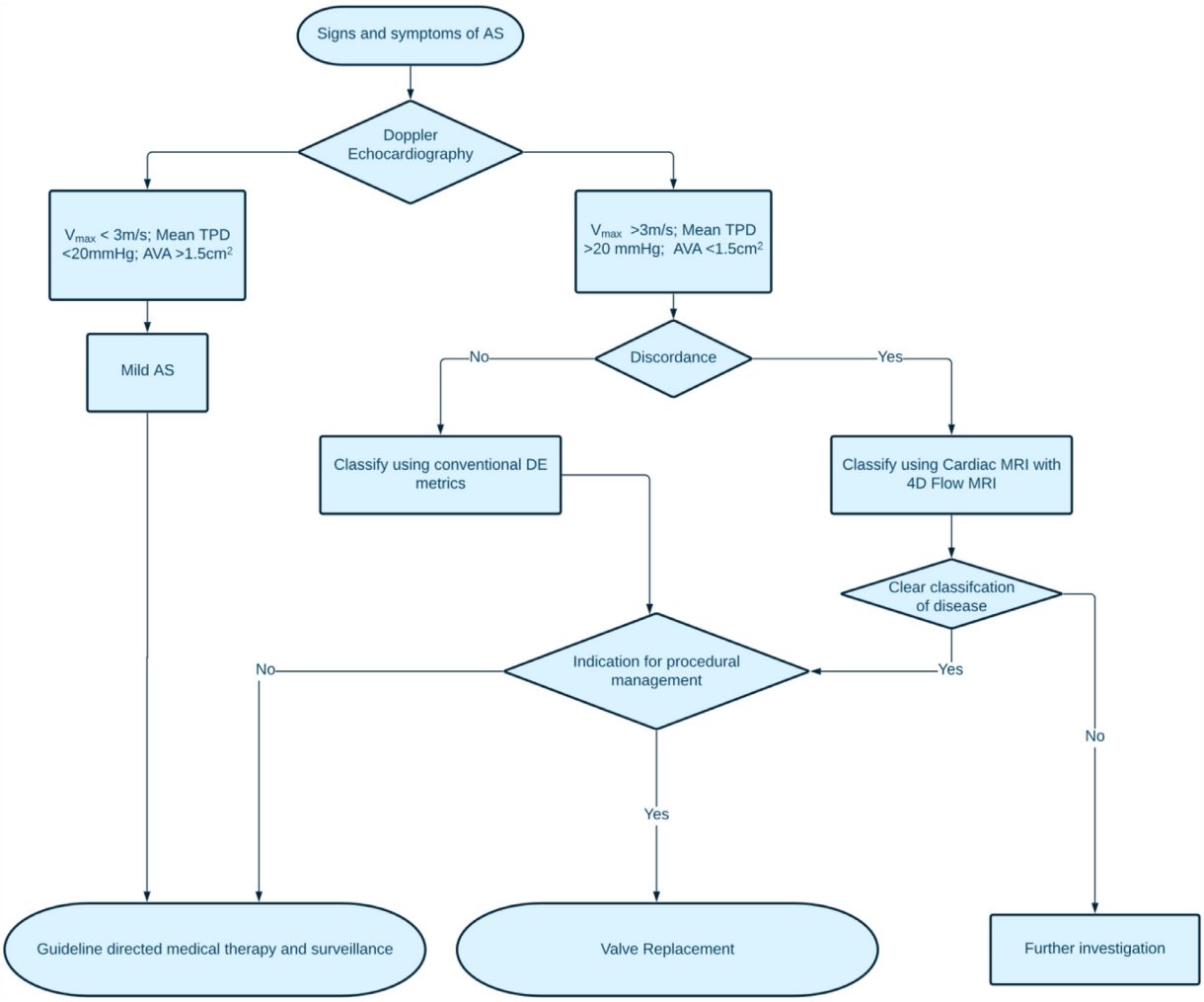

Fig. 4. The anticipated role of 4D flow MRI in the clinical assessment of aortic stenosis. 4D-flow MRI can be used alongside Doppler echocardiography and offers potential advantages beyond current guidelines. Further investigation (potentially including dobutamine stress echocardiography, stress-CMR, cardiac CT, serum biomarkers and exercise testing) is required in cases of continued uncertainty. Abbreviations: AS – aortic stenosis, AVA – aortic valve area, MRI – magnetic resonance imaging, TPD – transvalvular pressure drop, V_{max} – peak jet velocity

of the blood flow provides additional insight and a host of 4D-flow derived parameters may also have clinical significance [82].

Whilst many US velocity vector techniques either lack the capability or are limited to non-clinical systems, 4D-flow MRI is a validated method of acquiring 3D-velocity data on commercially available equipment. Despite this, 4D-flow MRI is not routinely undertaken and several factors account for this. DE is well-established as the gold-standard non-invasive test for diagnosis and surveillance of AS, with guideline-driven patient pathways and the infrastructure to support this at all levels of healthcare. On the other hand, despite increasing availability, access to and expertise in cardiac MRI is restricted to larger centres on account of the hardware and upkeep expenses, and the skilled personnel requisite for delivery and analysis. At present there is limited practicality for repeated scanning required for surveillance. Moreover, transthoracic echocardiography is used universally without contraindication, whereas MRI is unsuitable for patients suffering from claustrophobia or those with ferromagnetic or metallic implants. Body habitus may adversely impact image quality for DE, but may render MRI unfeasible if scanner bore is limiting. Furthermore, DE is fast with data and analysis available instantaneously, whereas long scanning times may preclude MRI in patients unable to tolerate lying supine for extended periods, although this can be minimised with the latest accelerated acquisition sequences [83]. Acquisition over several heart beats required for 4D flow MRI can lead to inaccuracy in patients with inconsistent R-R interval, although arguably DE suffers similarly requiring several measurements to account for beat-to-beat variation. Furthermore, prosthetic valve implants with metallic components are difficult to analyse using MRI due to metallic artefact, which is less of a limitation with DE.

Important technical considerations are necessary when integrating data into clinical decision-making. MRI suffers from partial volume averaging effects with underestimated velocity at the interface between blood and static tissue. Conversely, flow at the vessel wall is minute, thus impact to TPD calculations is likely to be minimal. Similar to 2D-phase contrast MRI, signal-to-noise ratio tends to fall at higher VENC settings, whilst lower settings risk aliasing – problems that may be mitigated by dual- or multi-VENC acquisition [84]. Reduced interobserver and intraobserver variability when compared with DE is a theoretical advantage and demonstrated in small cohorts but yet to be evaluated on a larger scale [59]. Most computational TPD techniques warrant segmentation of a ROI, however a great advantage of WERP and vWERP is that they minimise the impact of segmentation variability [76,85]. Whereas some techniques require substantial systems infrastructure for computation, SAW is less intensive than most NS-based techniques and provides rapidly with little computational cost as

velocity data is only required in a single observation plane, akin to 2D-PC MRI with 3 directional encoding [41].

Future work

The paucity of data is a significant barrier to more widespread usage of 4D flow MRI velocity data. Although validated for velocity, 4D-flow MRI derived pressure computations would ideally have direct comparison with transduced pressure data. Challenges of achieving this *in vivo* exist due to ethical considerations of the additional procedural risk. One way of overcoming this is the development of advanced phantom models suitable for multi-modality assessment. Our team has developed such a phantom comprising of a compliant valve and aorta circuit, with successful imaging with both ultrasound and MRI, and embedded pressure sensors for a non-damped, consistently positioned for direct transduction to complement non-invasive estimates [86].

To date no large scale trial has addressed the relative prognosticating power of 4D-flow MRI-derived measures, compared with invasive catheterisation and conventional DE. Undertaking a direct comparison between the three modalities is ethically unjustified except in selected groups, i.e. those that warrant cardiac catheterisation for other reasons, or at the time valve replacement, and in the latter of these groups the data may be biased for assessing prognosis. A prospective therapeutic trial comparing short- and intermediate- term outcomes based on DE-guided versus 4D-flow MRI-guided management for patients with discordant echocardiographic parameters may prove instructive and demonstrate a use case, although large numbers would be necessary to power the study due to the heterogeneity of the patient group. Further pilot work establishing normal values to delineate different degrees of severity required before such a trial could be undertaken. Standardisation of proprietary acquisition and post-processing tools is necessary to support multi-centre studies.

Emergent ultrasound techniques to capture more detailed velocity fields still require significant development. Much of the current data relate to carotid ultrasound or TEE (with limited depth penetration) and may not be applicable to transthoracic imaging or limited to transesophageal echocardiography. Where the aortic valve has been imaged, the signal-noise ratio prevented velocity estimation, although techniques to overcome this such as multi-velocity encoding, or coded excitation have been suggested [61]. Techniques providing out-of-plane velocity vector imaging usually require contrast and vast computation power. Progress with transducer technology is essential before translation into clinical cohorts [87].

Conclusions

The TPD is a key marker of the increased haemodynamic burden placed on the left ventricle. Despite widespread clinical use and a firm evidence base for the use of SB on DE data, there are opportunities to increase the accuracy and precision of current methods of measurement. Novel avenues of evaluation are emerging but require more work to establish normal values and utility beyond current techniques. Furthermore, developments in probe and processor technology will be necessary before preliminary techniques developed using 4D-flow MRI can be applied using cardiac ultrasound in everyday clinical practice.

Ethical statement

We the undersigned declare that this manuscript is original, has not been published before and is not currently being considered for publication elsewhere.

We confirm that the manuscript has been read and approved by all named authors and that there are no other persons who satisfied the criteria for authorship but are not listed. We further confirm that the order of authors listed in the manuscript has been approved by all of us.

We confirm that all authors are responsible for the content and have read and approved the manuscript; and that the manuscript conforms to the Uniform Requirements for Manuscripts Submitted to Biomedical Journals published in *Annals in Internal Medicine*

We understand that the Corresponding Author is the sole contact for the Editorial process. He is responsible for communicating with the other authors about progress, submissions of revisions and final approval of proofs.

Signed by all authors as follows:

Harminder Gill (Corresponding author, on behalf of all authors)

Conflicts of Interest

DN and PL are authors of patents protecting the technology to estimate accurate pressure differences from velocity fields (US Patent App. 16/707,310 and US Patent App. 16/085,258).

Funding

BHF Translational Award Ref: TG/17/3/33406; EU's Horizon 2020 R&I programme under the Marie Skłodowska-Curie g.a. No 764738; Wellcome Trust/EPSRC Centre for Medical Engineering (WT 203148/Z/16/Z); P.L. holds a Wellcome Trust Senior Research Fellowship (209450/Z/17/Z).

References

[1] Otto CM. Valvular aortic stenosis. disease severity and timing of intervention. J Am Coll Cardiol 2006;47:2141–51.
[2] Iung B, Vahanian A. Degenerative calcific aortic stenosis: A natural history. Heart 2012:98.
[3] Eveborn GW, Schirmer H, Heggelund G, Lunde P, Rasmussen K. The evolving epidemiology of valvular aortic stenosis. the Tromsø Study. Heart 2013;99:396–400.
[4] Dweck MR, Boon NA, Newby DE. Calcific aortic stenosis: A disease of the valve and the myocardium. J Am Coll Cardiol 2012;60:1854–63.
[5] Ito S, Miranda WR, Nkomo VT, Connolly HM, Pislaru SV, Greason KL, et al. Reduced left ventricular ejection fraction in patients with aortic stenosis. J Am Coll Cardiol 2018;71:1313–21.
[6] Otto CM, Nishimura RA, Bonow RO, Carabello BA, Iii JPE, Krieger E V, et al. 2020 ACC/AHA Guideline for the Management of Patients With Valvular Heart Disease. 2021.
[7] Vahanian A, Beyersdorf F, Praz F, Milojevic M, Baldus S, Bauersachs J, et al. 2021 ESC/EACTS Guidelines for the management of valvular heart disease Developed by the Task Force for the management of valvular heart disease of the European Society of Cardiology (ESC) and the European Association for Cardio-Thoracic Surgery (EACTS). Eur Heart J 2021.
[8] Carabello BA, Paulus WJ. Aortic stenosis. Lancet Elsevier Ltd 2009;373:956–66.
[9] Gorlin R, Gorlin SG. Hydraulic formula for calculation of the area of the stenotic mitral valve, other cardiac valves, and central circulatory shunts. I. Am Heart J 1951;41:1–29.
[10] Wyman RM, Safian RD, Portway V, Skillman JJ, Mckay RG, Baim DS. Current complications of diagnostic and therapeutic cardiac catheterization. J Am Coll Cardiol 1988;12:1400–6.
[11] Vahanian A, Baumgartner H, Bax J, Butchart E, Dion R, Filippatos G, et al. Guidelines on the management of valvular heart disease: The task force on the management of valvular heart disease of the European society of cardiology. Eur Heart J 2007;28:230–68.
[12] González-Mansilla A, Martinez-Legazpi P, Prieto A, Gomá E, Haurigot P, Pérez Del Villar C, et al. Valve area and the risk of overestimating aortic stenosis. Heart 2019;105:911–19.
[13] Bradley SM, Foag K, Monteagudo K, Rush P, Strauss CE, Gössl M, et al. Use of routinely captured echocardiographic data in the diagnosis of severe aortic stenosis. Heart 2019;105:112–16.
[14] Baumgartner H. Should we forget about valve area when assessing aortic stenosis? Heart 2019;105:92–3.
[15] Kanamori N, Taniguchi T, Morimoto T, Shiomi H, Ando K, Murata K, et al. Asymptomatic versus symptomatic patients with severe aortic stenosis. Sci Rep 2018;8:2–11.
[16] Rafique AM, Biner S, Ray I, Forrester JS, Tolstrup K, Siegel RJ. Meta-analysis of prognostic value of stress testing in patients with asymptomatic severe aortic stenosis. Am J Cardiol 2009;104:972–7 Elsevier Inc.

[17] Saeed S, Rajani R, Seifert R, Parkin D, Chambers JB. Exercise testing in patients with asymptomatic moderate or severe aortic stenosis. Heart 2018:1836–42.
[18] Berthelot-Richer M, Pibarot P, Capoulade R, Dumesnil JG, Dahou A, Thebault C, et al. Discordant grading of aortic stenosis severity: echocardiographic predictors of survival benefit associated with aortic valve replacement. JACC: Cardiovascular Imaging 2016;9:797–805.
[19] Pawade T, Clavel MA, Tribouilloy C, Dreyfus J, Mathieu T, Tastet L, et al. Computed tomography aortic valve calcium scoring in patients with aortic stenosis. Circulation: Cardiovascular Imaging 2018;11:1–11.
[20] Minners J, Allgeier M, Gohlke-Baerwolf C, Kienzle RP, Neumann FJ, Jander N. Inconsistent grading of aortic valve stenosis by current guidelines: Haemodynamic studies in patients with apparently normal left ventricular function. Heart 2010;96:1463–8.
[21] Annabi MS, Touboul E, Dahou A, Burwash IG, Bergler-Klein J, Enriquez-Sarano M, et al. Dobutamine stress echocardiography for management of low-flow, low-gradient aortic stenosis. J Am Coll Cardiol 2018;71:475–85.
[22] Clavel MA, Magne J, Pibarot P. Low-gradient aortic stenosis. Eur Heart J 2016;37:2645–57.
[23] Saikrishnan N, Kumar G, Sawaya FJ, Lerakis S, Yoganathan AP. Accurate assessment of aortic stenosis: A review of diagnostic modalities and hemodynamics. Circulation 2014;129:244–53.
[24] Laskey WK, Kussmaul WG. Pressure recovery in aortic valve stenosis. Circulation 1994;89:116–21.
[25] Pritchard P, Leylegian J. Fox and McDonald's Introduction to Fluid Mechanics. 2011.
[26] De Vecchi A, RE Clough, Gaddum NR, Rutten MCM, Lamata P, Schaeffter T, et al. Catheter-induced errors in pressure measurements in vessels: an In-vitro and numerical study Europe PMC funders group. IEEE Trans Biomed Eng 2014;61:1844–50.
[27] Sung HW, Yu PS, Hsu CH, Hsu JC. Can cardiac catheterization accurately assess the severity of aortic stenosis? An in vitro pulsatile flow study. Ann Biomed Eng 1997;25:896–905.
[28] Currie P, Seward J, Reeder G, Vlietstra R, Breshnahan D, Bresnahan J, et al. Continuous-wave doppler echocardiographic assessment of severity of calcific aortic stenosis: a simultaneous doppler-catheter correlative study in 100 adult patients. Circulation 1985;71:1162–9.
[29] Rajani R, Hancock J, Chambers JB. The art of assessing aortic stenosis. Heart BMJ Publishing Group Ltd Br Cardiovascular Soc 2012;98:iv14–22.
[30] Heinrich RS, Fontaine AA, Grimes RY, Sidhaye A, Yang S, Moore KE, et al. Experimental analysis of fluid mechanical energy losses in aortic valve stenosis: Importance of pressure recovery. Ann Biomed Eng 1996;24:685–94.
[31] Garcia D, Pibarot P, Dumesnil JG, Sakr F, Durand LG. Assessment of aortic valve stenosis severity: A new index based on the energy loss concept. Circulation 2000;101:765–71.
[32] Bahlmann E, Gerdts E, Cramariuc D, Gohlke-Baerwolf C, Nienaber CA, Wachtell K, et al. Prognostic value of energy loss index in asymptomatic aortic stenosis. Circulation 2013;127:1149–56.
[33] Heys JJ, Holyoak N, Calleja AM, Belohlavek M, Chaliki HP. Revisiting the simplified bernoulli equation. Open Biomed Eng J 2010;4:123–8.
[34] Hatle L, Angelsen BA, Tromsdal A. Non-invasive assessment of aortic stenosis by Doppler ultrasound. Br Med J 1980;43:284–92.
[35] Harris P, Kuppurao L. Quantitative Doppler echocardiography. BJA Education 2016;16:46–52.
[36] Zhang Y, Nitter-hauge S, Myhre E. Determination of the mean pressure gradient in aortic stenosis by doppler echocardiography. Eur Heart J 1985;6:999–1005.
[37] Bohbot Y, Rusinaru D, Delpierre Q, Marechaux S, Tribouilloy C. Risk stratification of severe aortic stenosis with preserved left ventricular ejection fraction using peak aortic jet velocity: an outcome study. Circulation: Cardiovascular Imaging 2017;10:1–9.
[38] Hatle L. Noninvasive assessment and differentiation of left ventricular outflow obstruction with Doppler ultrasound. Circulation 1981;64:381–7.
[39] Bohbot Y, Kowalski C, Rusinaru D, Ringle A, Marechaux S, Tribouilloy C. Impact of mean transaortic pressure gradient on long-term outcome in patients with severe aortic stenosis and preserved left ventricular ejection fraction. J Am Heart Assoc 2017;6.
[40] Rijsterborgh H, Roelandt J. Doppler assessment of aortic stenosis: Bernoulli revisited. Ultrasound Med Biol 1987;13:241–8.
[41] Donati F, Myerson S, Bissell MM, Smith NP, Neubauer S, Monaghan MJ, et al. Beyond bernoulli: improving the accuracy and precision of noninvasive estimation of peak pressure drops. Circulation: Cardiovascular Imaging 2017;10:1–9.
[42] Lamata P, Pitcher A, Krittian S, Nordsletten D, Bissell MM, Cassar T, et al. Aortic relative pressure components derived from four-dimensional flow cardiovascular magnetic resonance. Magn Reson Med 2014;72:1162–9.
[43] Binter C, Gotschy A, Sündermann SH, Frank M, Tanner FC, Lüscher TF, et al. Turbulent kinetic energy assessed by multipoint 4-dimensional flow magnetic resonance imaging provides additional information relative to echocardiography for the determination of aortic stenosis severity. Circulation: Cardiovascular Imaging 2017;10.
[44] Levine RA, Jimoh A, Cape EG, McMillan S, Yoganathan AP, Weyman AE. Pressure recovery distal to a stenosis: Potential cause of gradient "overestimation" by Doppler echocardiography. J Am Coll Cardiol 1989;13:706–15.
[45] Pibarot P, Garcia D, Dumesnil JG. Energy loss index in aortic stenosis: From fluid mechanics concept to clinical application. Circulation 2013;127:1101–4.
[46] Gilon D, Cape EG, Handschumacher MD, Song JK, Solheim J, VanAuker M, et al. Effect of three-dimensional valve shape on the hemodynamics of aortic stenosis: Three-dimensional echocardiographic stereolithography and patient studies. J Am Coll Cardiol 2002;40:1479–86.
[47] Abbas AE, Franey LM, Lester S, Raff G, Gallagher MJ, Hanzel G, et al. The role of jet eccentricity in generating disproportionately elevated transaortic pressure gradients in patients with aortic stenosis. Echocardiography 2015;32:372–82.
[48] Baumgartner H, Hung J, Bermejo J, Chambers JB, Edvardsen T, Goldstein S, et al. Recommendations on the echocardiographic assessment of aortic valve stenosis: A focused update from the European Association of Cardiovascular Imaging and the American Society of Echocardiography. Eur Heart J Cardiovascular Imaging 2017;18:254–75.
[49] Kitzman DW. Normal age-related changes in the heart: Relevance to echocardiography in the elderly. Am J Geriatric Cardiol 2000;9:311–20.
[50] Ebbers T, Wigström L, Bolger AF, Engvall J, Karlsson M. Estimation of relative cardiovascular pressures using time-resolved three-dimensional phase contrast MRI. Magn Reson Med 2001;45:872–9.
[51] van Dijk P. Direct cardiac NMR imaging of heart wall and blood flow velocity. J Comput Assist Tomogr 1984;8:429–36.
[52] Markl M, Frydrychowicz A, Kozerke S, Hope M, Wieben O. 4D flow MRI. J Magn Reson Imaging 2012;36:1015–36.
[53] Loecher M, Schrauben E, Johnson KM, Wieben O. Phase unwrapping in 4D MR flow with a 4D single-step laplacian algorithm. J Magn Reson Imaging 2016;43:833–42.
[54] Adriaans BP, Westenberg JJM, Cauteren YJM, van, Gerretsen S, Elbaz MSM, Bekkers SCAM, et al. Clinical assessment of aortic valve stenosis: Comparison between 4D flow MRI and transthoracic echocardiography. J Magn Reson Imaging 2020;51:472–80.
[55] Garcia J, Kadem L, Larose E, Clavel MA, Pibarot P. Comparison between cardiovascular magnetic resonance and transthoracic doppler echocardiography for the estimation of effective orifice area in aortic stenosis. J Cardiovasc Magn Reson 2011;13:1–9.
[56] Stam K, Chelu RG, der Velde N van, van Duin R, Wielopolski P, Nieman K, et al. Validation of 4D flow CMR against simultaneous invasive hemodynamic measurements: a swine study. Int J Cardiovasc Imaging Springer Netherlands 2019;35:1111–18.
[57] Levy F, Iacuzio L, Civaia F, Rusek S, Dommerc C, Hugues N, et al. Usefulness of 3-Tesla cardiac magnetic resonance imaging in the assessment of aortic stenosis severity in routine clinical practice. Arch Cardiovasc Dis 2016;109:618–25.
[58] Rose MJ, Jarvis K, Chowdhary V, Barker AJ, Allen BD, Robinson JD, et al. Efficient method for volumetric assessment of peak blood flow velocity using 4D flow MRI. J Magn Reson Imaging 2016;44:1673–82.
[59] Archer GT, Elhawaz A, Barker N, Fidock B, Rothman A, der Geest RJ van, et al. Validation of four-dimensional flow cardiovascular magnetic resonance for aortic stenosis assessment. Sci Rep 2020;10:1–10.
[60] Lantz J, Gupta V, Henriksson L, Karlsson M, Persson A, Carlhäll C-J, et al. Intracardiac Flow at 4D CT: Comparison with 4D Flow MRI. Radiology 2018;289:51–8.
[61] Hansen KL, Nielsen MB, Jensen JA. Vector velocity estimation of blood flow – A new application in medical ultrasound. Ultrasound 2017;25:189–99.
[62] Løvstakken L, Lie GR. BSI (Blood Speckle Imaging). 2021
[63] Geyer H, Caracciolo G, Abe H, Wilansky S, Carerj S, Gentile F, et al. Assessment of myocardial mechanics using speckle tracking echocardiography: fundamentals and clinical applications. J Am Soc Echocardiogr 2010;23:351–69.
[64] Wigen MS, Fadnes S, Rodriguez-Molares A, Bjåstad T, Eriksen M, Stensæth KH, et al. 4-D intracardiac ultrasound vector flow imaging-feasibility and comparison to phase-contrast MRI. IEEE Trans Med Imaging 2018;37:2619–26269.
[65] Zhou X, Leow CH, Rowland E, Riemer K, Rubin JM, Weinberg PD, et al. 3-D velocity and volume flow measurement in vivo using speckle decorrelation and 2-D high-frame-rate contrast-enhanced ultrasound. IEEE Trans Ultrason Ferroelectr Freq Control 2018;65:1–12.
[66] Olesen JB, Villagomez-Hoyos CA, Moller ND, Ewertsen C, Hansen KL, Nielsen MB, et al. Noninvasive estimation of pressure changes using 2-D vector velocity ultrasound: an experimental study with In vivo examples. IEEE Trans Ultrason Ferroelectr Freq Control 2018;65:709–19.
[67] Barker AJ, van Ooij P, Bandi K, Garcia J, Albaghdadi M, McCarthy P, et al. Viscous energy loss in the presence of abnormal aortic flow. Magn Reson Med 2014;72:620–8.
[68] Clark C. Turbulent velocity measurements in a model of aortic stenosis. J Biomech 1976;9:677–87.
[69] Stein PD, Sabbah HN. Turbulent blood flow in the ascending aorta of humans with normal and diseased aortic valves. Circ Res 1976;39:58–65.
[70] Dyverfeldt P, Hope MD, Tseng EE, Saloner D. Magnetic resonance measurement of turbulent kinetic energy for the estimation of irreversible pressure loss in aortic stenosis. JACC: Cardiovascular Imaging 2013;6:64–71 Elsevier Inc.
[71] Gore JC. Turbulent flow effects on NMR imaging: measurement of turbulent intensity. Med Phys 1991;18:1045–51.
[72] Dyverfeldt P, Gårdhagen R, Sigfridsson A, Karlsson M, Ebbers T. On MRI turbulence quantification. Magn Reson Imaging 2009;27:913–22 Elsevier Inc.
[73] Binter C, Gülan U, Holzner M, Kozerke S. On the accuracy of viscous and turbulent loss quantification in stenotic aortic flow using phase-contrast MRI. Magn Reson Med 2016;76:191–6.
[74] Ha H, Lantz J, Ziegler M, Casas B, Karlsson M, Dyverfeldt P, et al. Estimating the irreversible pressure drop across a stenosis by quantifying turbulence production using 4D Flow MRI. Scientific Reports Nature Publishing Group 2017;7:1–14.
[75] Donati F, Figueroa CA, Smith NP, Lamata P, Nordsletten DA. Non-invasive pres-

sure difference estimation from PC-MRI using the work-energy equation. Med Image Anal 2015;26:159–72 Elsevier Ltd.
[76] Marlevi D, Ha H, Dillon-Murphy D, Fernandes JF, Fovargue D, Colarieti-Tosti M, et al. Non-invasive estimation of relative pressure in turbulent flow using virtual work-energy. Med Image Anal 2020;60:101627 Elsevier B.V.
[77] Bahlmann E, Cramariuc D, Gerdts E, Gohlke-Baerwolf C, Nienaber CA, Eriksen E, et al. Impact of pressure recovery on echocardiographic assessment of asymptomatic aortic stenosis: A SEAS substudy. JACC: Cardiovascular Imaging 2010;3:555–62 Elsevier Inc.
[78] Zoghbi WA, Farmer KL, Soto JG, Nelson JG, Quinones MA. Accurate noninvasive quantification of stenotic aortic valve area by Doppler echocardiography. Circulation 1986;73:452–9.
[79] Yang CS, Marshall ES, Fanari Z, Kostal MJ, West JT, Kolm P, et al. Discrepancies between direct catheter and echocardiography-based values in aortic stenosis. Catheter Cardiovasc Interv 2016;87:488–97.
[80] Geske JB, Cullen MW, Sorajja P, Ommen SR, Nishimura RA. Assessment of Left Ventricular Outflow Gradient Hypertrophic Cardiomyopathy Versus Aortic Valvular Stenosis. JACC: Cardiovascular Interventions. Elsevier Inc; 2012.
[81] Fatehi Hassanabad A, Burns F, Bristow MS, Lydell C, Howarth AG, Heydari B, et al. Pressure drop mapping using 4D flow MRI in patients with bicuspid aortic valve disease: A novel marker of valvular obstruction. Magnetic Resonance Imaging Elsevier 2020;65:175–82.
[82] Garcia J, Barker AJ, Markl M. The role of imaging of flow patterns by 4D flow MRI in aortic stenosis. JACC: Cardiovascular Imaging 2019;12:252–66.
[83] Pathrose A, Ma L, Berhane H, Scott MB, Chow K, Forman C, et al. Highly accelerated aortic 4D flow MRI using compressed sensing: Performance at different acceleration factors in patients with aortic disease. Magn Reson Med 2021;85:2174–87 John Wiley & Sons, Ltd.
[84] Ma LE, Markl M, Chow K, Vali A, Wu C, Schnell S. Efficient triple - VENC phase - contrast MRI for improved velocity dynamic range. Magentic Resonance Med 2019;00:1–16.
[85] Marlevi D, Ruijsink B, Balmus M, Dillon-Murphy D, Fovargue D, Pushparajah K, et al. Estimation of cardiovascular relative pressure using virtual work-energy. Sci Rep 2019;9:1–16.
[86] Gill H, Fernandes JF, Bissell M, Wang S, Sotelo J, Urbina J, et al. 3D printed valve models replicate in vivo bicuspid aortic valve peak pressure drops. J Am Coll Cardiol Am Coll Cardiol Foundation 2016;67:1611.
[87] ter Haar G. Safety and bio-effects of ultrasound contrast agents. Med Biol Eng Comput 2009;47:893–900.
[88] Casas B, Lantz J, Dyverfeldt P, Ebbers T. 4D Flow MRI-based pressure loss estimation in stenotic flows: Evaluation using numerical simulations. Magn Reson Med 2016;75:1808–21.
[89] Haraldsson H, Kefayati S, Ahn S, Dyverfeldt P, Lantz J, Karlsson M, et al. Assessment of Reynolds stress components and turbulent pressure loss using 4D flow MRI with extended motion encoding. Magn Reson Med 2018;79:1962–71.